

Thermoreversible Gelation of Poly(vinylidene fluoride) in Diesters: Influence of Intermittent Length on Morphology and Thermodynamics of Gelation

Asok K. Dikshit and Arun K. Nandi*

Polymer Science Unit, Indian Association for the Cultivation of Science, Jadavpur, Calcutta, 700032, India

Received June 4, 1999; Revised Manuscript Received December 2, 1999

ABSTRACT: Poly(vinylidene fluoride) (PVF₂) produces thermoreversible gels in diesters. By variation of the number of intermittent carbon atoms ($n = 0-7$) of the diesters, the physical properties of the gels are studied. The morphology of the PVF₂/diethyl oxalate (DEO) gel is spheroidal, but the morphology of PVF₂/diethyl malonate (DEM) gel is a mixture of both spheroidal and fibrillar. The PVF₂/diethyl succinate (DES), PVF₂/diethyl glutarate (DEG), PVF₂/diethyl pimelate (DEP), and PVF₂/diethyl azelate (DEAZ) gels are "fibrillar-like" as evidenced from scanning electron microscopy (SEM) and transmission electron microscopy (TEM). The X-ray and solvent subtracted FT-IR spectra indicate the presence of α -polymorph PVF₂ in all the gels. The enthalpy of gel formation and the enthalpy of gel fusion, measured from differential scanning calorimetry (DSC), show linear plot with PVF₂ concentration for PVF₂-DEO gels but others exhibit positive deviation from linearity. From the deviation vs PVF₂ weight fraction (W_{PVF_2}) plot, the compositions of the polymer solvent complexes are found to be 1:3, 1:2, 1:4, 1:4, and 1:3 in the molar ratio of the diester and PVF₂ repeating unit, for gels in DEM, DES, DEG, DEP, and DEAZ, respectively. The phase diagrams of PVF₂-DEM, PVF₂-DES, and PVF₂-DEP gels indicate polymer-solvent compound formation with a singular point while those of the PVF₂-DEG and PVF₂-DEAZ gels indicate compound formation with an incongruent melting point. The polymer solvent compound formation is also studied by molecular mechanics calculations using MMX program. The pairs of α -PVF₂ and diester molecules with appropriate conformation to match the composition of the complex are energetically minimized. The distances between the $>\text{CF}_2$ group and the carbonyl oxygen are lower than the summation of their van der Waals radii for all the diesters. The discrepancy between molecular modeling and morphology of the PVF₂-DEO gels and the borderline morphology of PVF₂-DEM gels have been explained from molecular mobility of the solvent and enthalpy of complexation (ΔH_c). The gel melting temperature and gelation temperature increases with increase in intermittent length (n) for a particular PVF₂ concentration. Also, ΔH_c increases with " n ", and this indicates that the intermittent length of diesters has both enthalpic and entropic contribution on gel behavior of PVF₂.

Introduction

Thermoreversible polymer gels have drawn considerable interest for the past few years.^{1,2} A few thermoreversible poly(vinylidene fluoride) (PVF₂) gels are also reported in different solvents because of the technological importance of PVF₂ for its piezo- and pyroelectric properties.³ The PVF₂ gels exhibit two different morphologies, spheroidal and fibrillar, in these gels.⁴⁻⁸ Recently, it is shown by some researchers that fibrillar gels display elastic properties while the spheroidal gels do not.⁹ PVF₂ can crystallize in five different polymorphs, e.g., α , β , γ , δ and ϵ , of which α is the most common polymorph.¹⁰ The α polymorph has a TGTG conformation, the β polymorph has an all-trans conformation, γ polymorph has a T₃GT₃G conformation, and δ and ϵ polymorphs are polar and antipolar analogues of the α and γ forms.¹⁰

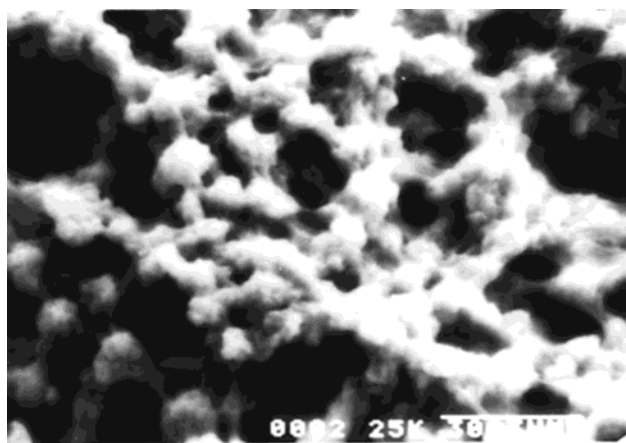
Earlier we have observed that PVF₂ gels in diethyl adipate with fibrillar morphology having α -polymorph crystals.⁸ It is now believed that the solvent has a strong involvement in the gelation process.² However, there exists no report where the nature of the interaction of the solvent with the polymer is kept the same but where the distance of interacting groups and the molecular weight of the solvent are varied. In this paper, we would like to concentrate on the formation of PVF₂ gels in diesters with varying intermittent ($-\text{CH}_2-$) _{n} length. The work is chosen to see if by varying the intermittent

length ($n = 0-7$) (so too the molecular weight), the morphology, structure, and thermodynamics of the PVF₂ gel can be changed. An attempt is made to correlate the morphology with the thermodynamics of gelation. Here the attempt has been made to explain the gel behavior of PVF₂ with the diesters by the molecular mechanics calculations (MMX method).

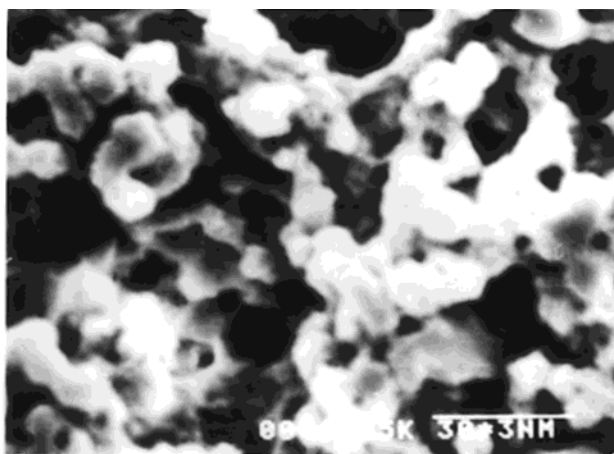
Experimental Section

Samples. A commercial PVF₂ sample (KY-201, Pennwalt Corp.) was recrystallized from its dilute solution (0.3% w/v) in acetophenone, washed with methanol and dried in a vacuum at 60 °C for 3 days. The weight-average molecular weight (M_w) of the sample was 8.81×10^5 , polydispersity index (PDI) = 2.82, and head to head (H-H) defect = 5.31 mol %.⁸ The solvents, diethyl oxalate (DEO) [Berguin] and diethyl malonate (DEM) [Berguin] were distilled under reduced pressure whereas diethyl succinate (DES), diethyl glutarate (DEG), diethyl pimelate (DEP) and diethyl azelate (DEAZ) were received from Lancaster and were used as received.

Preparation of Gel. The gels were prepared in two ways: (1) For morphology and structural investigation, the gels were prepared 6% (w/v) in glass tubes (8 mm i.d.) by taking an appropriate amount of polymer and solvent. The tubes were degassed by the repeated freeze-thaw technique and were sealed under vacuum (10^{-3} mmHg). They were made homogeneous at 180 °C and were quickly gelled by quenching at room temperature (30 °C). (2) For thermodynamic study, the gels were prepared in Perkin-Elmer large volume capsules (LVC) by taking appropriate amounts of polymer and solvent,



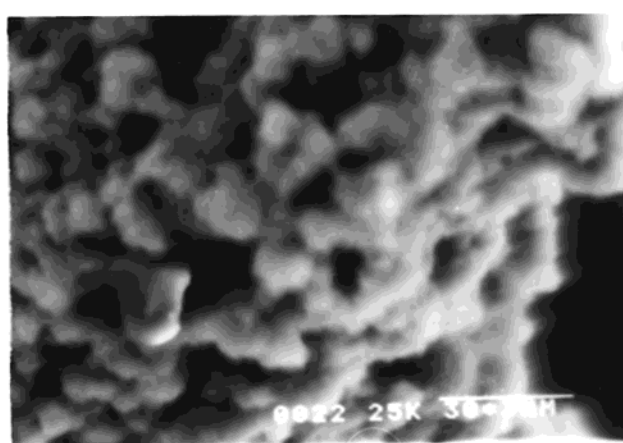
(a)



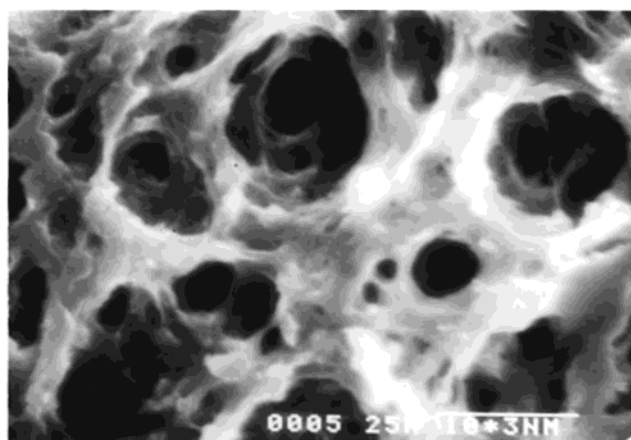
(b)



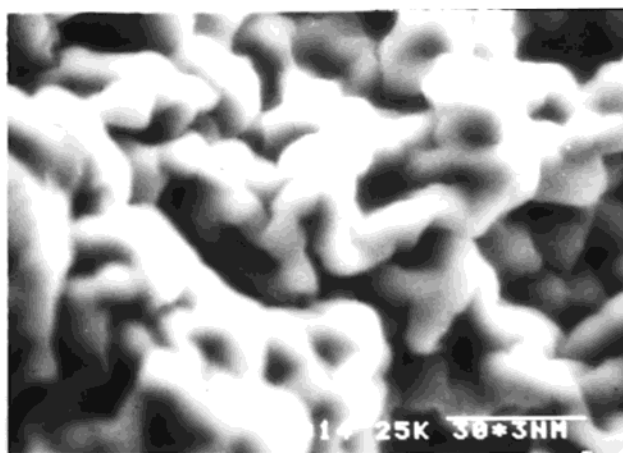
(c)



(d)



(e)



(f)

Figure 1. SEM pictures of 6% (w/v) dried PVF₂ gel in diesters: (a) DEO, (b) DEM, (c) DES, (d) DEG, (e) DEP, and (f) DEAZ. (The scale in each micrograph indicates 30×10^3 nm.)

and the capsules were tightly sealed with the help of a quick press. They were subsequently made homogeneous by keeping them at 180 °C in DSC for 10 min with occasional shaking and gelled at 20 °C for 20 min by cooling from 180 °C at the rate of 200 °C/min.

Morphological and Structural Investigation. The morphology of the gels were investigated using both scanning electron microscopy (SEM) and transmission electron microscopy (TEM). For scanning electron microscopy the 6% (w/v)

gels were dried in a vacuum at room temperature and were gold coated. Their scanning electron micrographs were then taken in a SEM apparatus (Hitachi S-415A). The TEM study was done by dropping 0.3% (w/v) solution of PVF₂ in diesters directly on a carbon coated copper grid, which was then dried at 30 °C under vacuum for 3 days. The gels were then observed in a transmission electron microscope (Hitachi H-600).

The structural investigations of the gels were done by wide-angle X-ray scattering (WAXS) and Fourier transformed

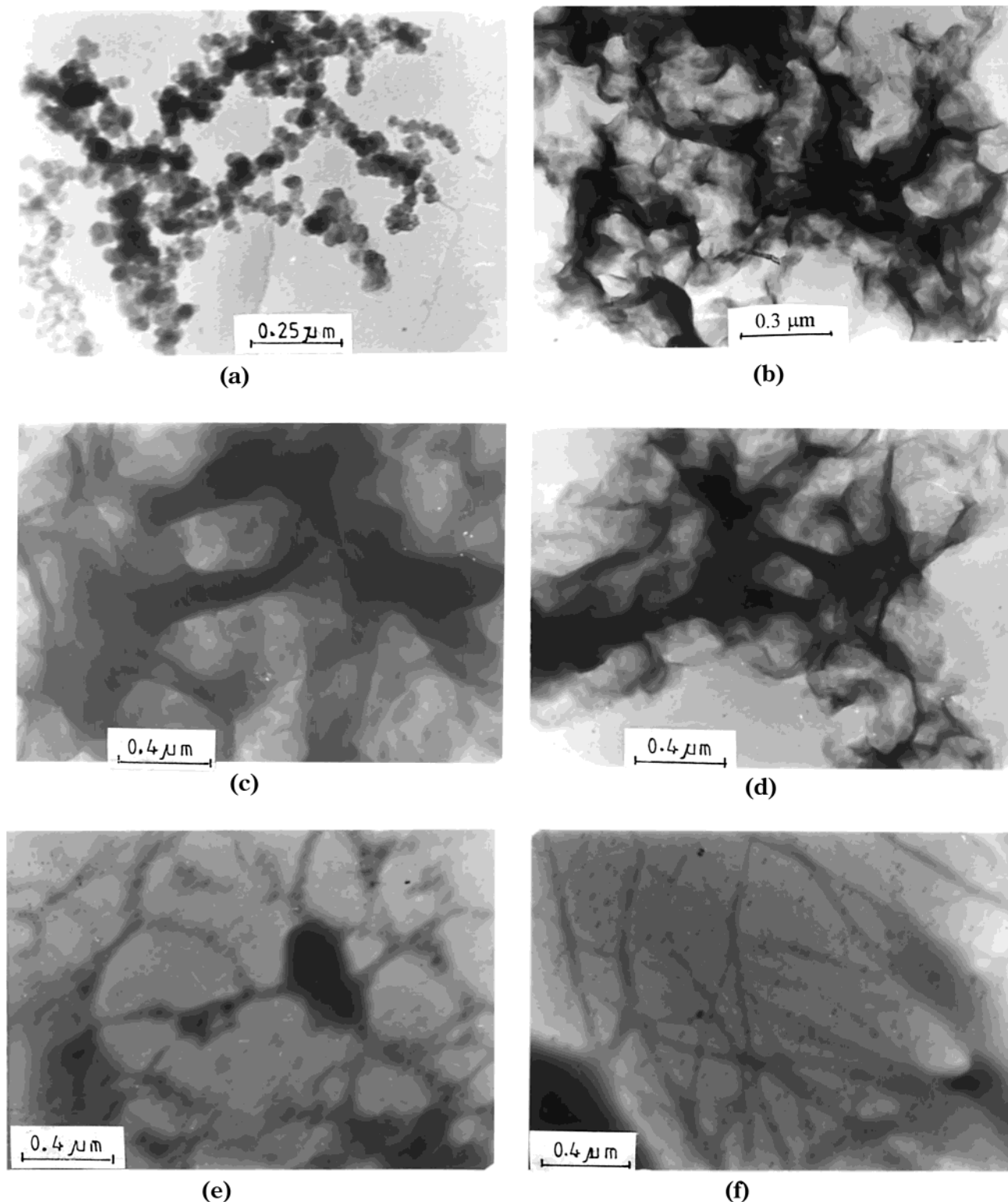


Figure 2. TEM pictures of 0.3% (w/v) PVF₂ gel in diesters: (a) DEO, (b) DEM, (c) DES, (d) DEG, (e) DEP, and (f) DEAZ.

infrared spectroscopy (FT-IR) methods. In the WAXS study, the gels were dried in a vacuum at 35 °C for 1 month, and the diffractograms were recorded in a Philips powder diffraction apparatus (model PW1710). Nickel-filtered Cu K α radiation was used, and the diffractograms of the gels were recorded at the scanning rate of 0.09° 2 θ /min. The FT-IR study was done using a Nicolet FT-IR instrument [Magna IR750 spectrometer (Series-II)]. The solvents spectra were subtracted from the gel spectra to get the PVF₂ spectra in the gel from using a computer attached to the instrument.

Thermodynamic Study. The thermodynamic study of the gels was done in a Perkin-Elmer DSC-7 instrument. The gels

were made in LVC capsules, and before each run they were melted at 180 °C for 10 min and quenched to 20 °C in DSC for 20 min. They were then heated at the scan rate of 40°/min. The higher heating rate was chosen to avoid melt recrystallization during the heating process.^{7,8,11} The peak temperature and the enthalpy of gel melting were measured from the endotherm using a computer attached to the instrument. The enthalpy of gel formation and the gelation temperature were measured using a dynamic cooling method. In this method the LVC pan was cooled at the rate of 5°/min from 180 to 20 °C. From the endotherms the gelation temperature and enthalpy of gelation were measured from the computer attached to the

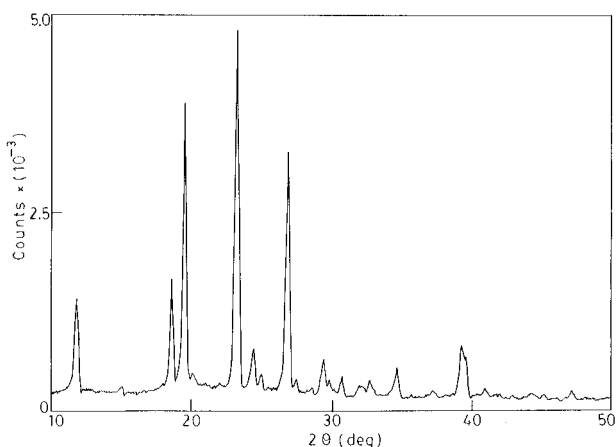


Figure 3. Representative WAXS pattern of 6% (w/v) PVF₂ gel (dried) in DEP.

instrument. The DSC was calibrated with indium before each set of experiment.

Results

Morphology. The PVF₂ gel in diethyl oxalate (DEO) is turbid, but the gels in diethyl malonate (DEM), diethyl succinate (DES), diethyl glutarate (DEG), diethyl pimelate (DEP), and diethyl azelate (DEAZ) are transparent. Figure 1 presents the scanning electron micrographs of 6% PVF₂ gels (dried) in different diesters. It is apparent from the figure that the PVF₂/DEO gel has spheroidal morphology; the PVF₂/DEM gel has a borderline morphology of both spheroidal and fibrillar in nature, and the other gels, e.g., PVF₂/DES, PVF₂/DEG, PVF₂/DEP and PVF₂/DEAZ gels, have no spheroidal morphology but are fibrillar-like. It is necessary to mention that PVF₂/diethyl adipate (DEA) gel has also fibrillar morphology.⁸ In Figure 2, the TEM pictures of the above gels are shown. It is also clear from the figure that except for the PVF₂/DEO gel all the other gels have fibrillar-like morphology. However, PVF₂/DEM gels

have a mixture of both spheroidal and fibrillar morphology. Thus, the TEM pictures closely resemble the SEM pictures, which are at much lower magnification than those of the former. It is apparent from Figure 2 that the texture of the fibrils becomes more distinct with an increase in the value of the intermittent carbon atoms (*n*). Of course, the morphology presented here is for the dried gels. So it is assumed throughout the paper that the undried gels also have a similar morphology.

Structure. The structure of the gels is determined from the WAXS pattern of the dried gel. A representative WAXS pattern of the PVF₂ gel (dried) is shown in Figure 3 for 6% PVF₂/DEP gel. From the figure, it is clear that the WAXS pattern corresponds to the α -polymorph of PVF₂.^{12–14} The WAXS patterns of the other gels also correspond to that of the α -polymorph only. In Table 1, the observed d_{hkl} values are compared for the dried PVF₂ gels from different solvents and also with that of the melt crystal (α -polymorph) of PVF₂.¹³ It is apparent from the table that some new d_{hkl} values are observed in the gels than those in the melt crystal. Also the intensity values for diffraction at different planes are compared relative to that of the 110 peak in each sample. Except in few cases, the intensity values do not tally exactly with those of the melt crystal. It indicates that although crystal system and *d* spacing remain the same, the atomic positions of the statistical up and down arrangement of the chains in the unit cell may somewhat be changed. So it may be surmised that the atomic coordinates in the unit cell are disturbed during gelation, and it may be due to the polymer–solvent complex formation discussed in the following section. The occurrence of the new peaks as shown by a superscript *a* in Table 1 may also be due to the solvated structure of α -PVF₂, as observed in the IPS gels.¹⁵

To investigate if there is any change in polymorphic structure during drying, we have performed solvent-subtracted FTIR spectra of the PVF₂ gels in diesters, and a representative FTIR spectra is shown in Figure 4. The peak positions of the subtracted spectra of PVF₂

Table 1. Comparison of d_{hkl} (Å) and Intensity Ratio of PVF₂–Diester Gels [d_{hkl}^{calc} for α -Phase PVF₂, with $a = 5.02$ Å, $b = 9.63$ Å, and $c = 4.62$ Å]

<i>hkl</i>	d_{hkl}^{calc}	I_{hkl}^0/I_{110}^0 mel crys	DEO		DEM		DES		DEG		DEP		DEAZ	
			d_{hkl}	I_{hkl}^0/I_{110}^0	d_{hkl}	I_{hkl}^0/I_{110}^0	d_{hkl}	I_{hkl}^0/I_{110}^0	d_{hkl}	I_{hkl}^0/I_{110}^0	d_{hkl}	I_{hkl}^0/I_{110}^0	d_{hkl}	I_{hkl}^0/I_{110}^0
									7.37 ^a	0.08	7.45 ^a	0.30		
					5.32 ^a	0.42								
					5.22 ^a	0.13								
100	5.02	0.52			4.95	0.31	5.05	0.42	4.98	0.39			5.00	0.41
020	4.81	0.64	4.87	0.50	4.75	0.54	4.86	0.57	4.77	0.60	4.75	0.40	4.82	0.80
													4.67 ^a	1.08
110	4.45	1.00	4.50	1.00	4.39	1.00	4.48	1.00	4.40	1.00	4.53	1.0	4.48	1.00
011	4.17	0.17											4.27 ^a	0.55
							3.48 ^a	0.24	3.63 ^a	0.10	3.81 ^a	1.25	3.90 ^a	0.74
									3.45 ^a	0.24	3.65 ^a	0.16		
											3.62 ^a	0.12		
021														
101	3.33	0.70	3.09	0.51	3.38	0.29	3.33	0.24	3.32	0.30	3.31	0.84	3.29	0.51
					3.24 ^a	0.17					3.02 ^a	0.13		
121	2.79	0.41	2.90	0.15					2.78	0.08			2.76	0.10
130	2.70	0.48	2.58	0.15	2.72	0.10	2.72	0.09						
200	2.51	0.54	2.52	0.15	2.50	0.24	2.42	0.58	2.48	0.07	2.58	0.10		
									2.40 ^a	0.11				
131	2.33	0.52	2.33	0.57	2.32	0.10	2.32	0.10	2.31	0.15	2.30	0.17	2.28	0.10
											2.27 ^a	0.12		
211	2.15	0.51	2.12	0.15			2.09	0.77						
041														
230	1.98	0.19			1.97	0.05	1.97	0.06	1.96	0.07				

^a Indicates the new peaks observed in the gels.

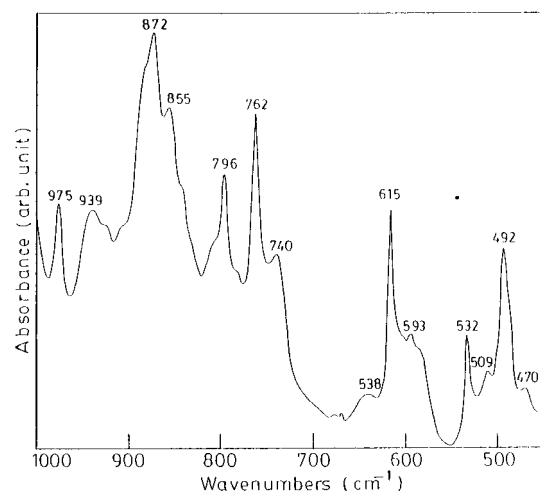


Figure 4. Representative solvent-subtracted FT-IR spectra of 6% (w/v) PVF₂ gel in DEP.

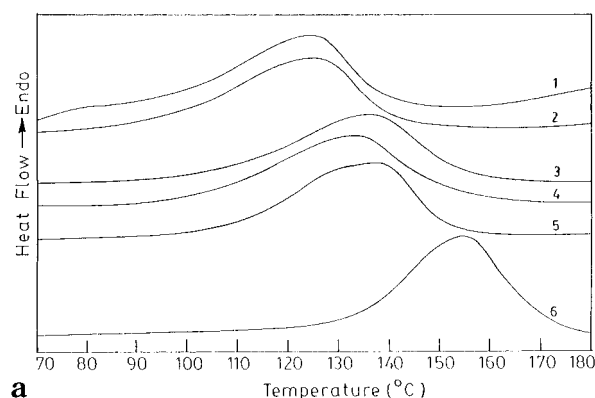
Table 2. FT-IR Peak Positions (cm⁻¹) of PVF₂ in its Gels with Diesters (Solvent Subtracted)

PVF ₂		DEO	DEM	DES	DEG	DEP	DEAZ
theor	soln cryst						
977	978	977	975	975	976	975	975
945	945		945	953	941	939	
				924 ^a			
907		911		902			
			884 ^a				880 ^a
877	876	871		870	873	872	872
855		855	856	855		855	854
842	848				845		841
			833 ^a				
795	798	795	796	795	796	796	796
762	763	761	762	762	762	762	762
			680 ^a		667 ^a	740 ^a	729 ^a
			644 ^a	639 ^a	636 ^a	638 ^a	
			633 ^a		627 ^a		
614	614	614	614	614	614	615	615
			571 ^a	567 ^a		593 ^a	
532	533	532	532	532	532	532	532
510			510	510	511	509	510
490	487	490	491	491	489	492	492
485		481	475				
470		465		470	468	470	

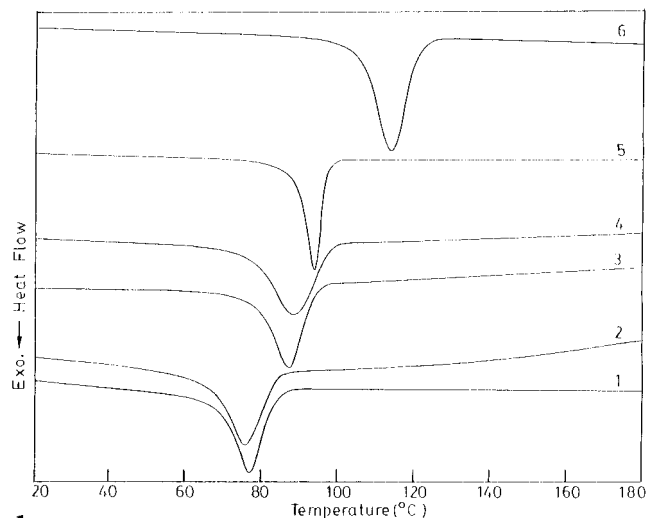
^a New peaks may be due to polymer-solvent complex formation.

gels studied here are presented in Table 2. From the table, it is clear that all of the spectra have a peak at 532 cm⁻¹ and this corresponds to the α -polymorph of PVF₂ with TGTG conformation.¹⁶⁻¹⁹ Thus, in all the gels, an α -polymorph PVF₂ crystal is produced, and from a WAXS study of dried gels, the same is also found. This proves that there is no change in the polymorphic structure of the crystal during the drying of the gels.

In Table 2 the position of the IR peaks of the subtracted spectra are compared with those of the pure PVF₂. It is clear from the table that except for the PVF₂/DEO gel, the other gels have some new peaks. For example the PVF₂-DEM system has new peaks at 884, 833, 680, 644, 633 and 571 cm⁻¹, the PVF₂-DES system has new peaks at 924, 639 and 567 cm⁻¹, the PVF₂-DEG system has new peaks at 667, 636 and 627 cm⁻¹, the PVF₂-DEP system has peaks at 740, 638, and 593 cm⁻¹ and the PVF₂-DEAZ system has peaks at 880 and 729 cm⁻¹. These new peaks may originate from the polymer-solvent complex formation in the gel form of PVF₂. A complete idea of the polymer-solvent complex



a



b

Figure 5. (a) DSC thermograms of PVF₂ gel in diesters prepared at 20 °C for 20 min and heated at the heating rate of 40 °C/min: (1) DEO ($W_{\text{PVF}_2} = 0.52$); (2) DEM ($W_{\text{PVF}_2} = 0.48$); (3) DES ($W_{\text{PVF}_2} = 0.5$); (4) DEG ($W_{\text{PVF}_2} = 0.52$); (5) DEP ($W_{\text{PVF}_2} = 0.48$); (6) DEAZ ($W_{\text{PVF}_2} = 0.55$). (b) DSC thermograms of PVF₂ gel in diesters, cooled from 180 °C at 5 °C/min. The numbers denote the same as in Figure 5a.

formation will be obtained from the thermodynamic study of the gels in the following section.

Thermodynamic Study

The representative DSC thermograms of each solvent are presented in Figure 5a for the gel melting and in Figure 5b for the gel formation process. It is apparent from the figures that each thermogram consists of single peak, and this is true for all compositions. In Figure 6a-f, the enthalpy of fusion and the enthalpy of gelation of all of the gels are plotted with weight fraction of PVF₂ (W_{PVF_2}). At the temperature of interest (20 °C), the solvents do not crystallize so that the ΔH of the solvent is considered as zero. In Figure 6a all the data points can be represented well by a straight line connecting ΔH of the solvent and that of the polymer. But in the other five cases we observe positive deviation from linearity joining those of the pure components in each plot. The enthalpy of gel melting may be considered to consist of three contributions:⁸

$$\Delta H^{\text{(per gm)}} = W_1 \Delta H_1 + W_2 \Delta H_2 + \Delta H_c \quad (1)$$

where W represents the weight fraction and subscripts 1 and 2 represent the diester and the PVF₂, respectively, ΔH_i represents the melting enthalpy of each component

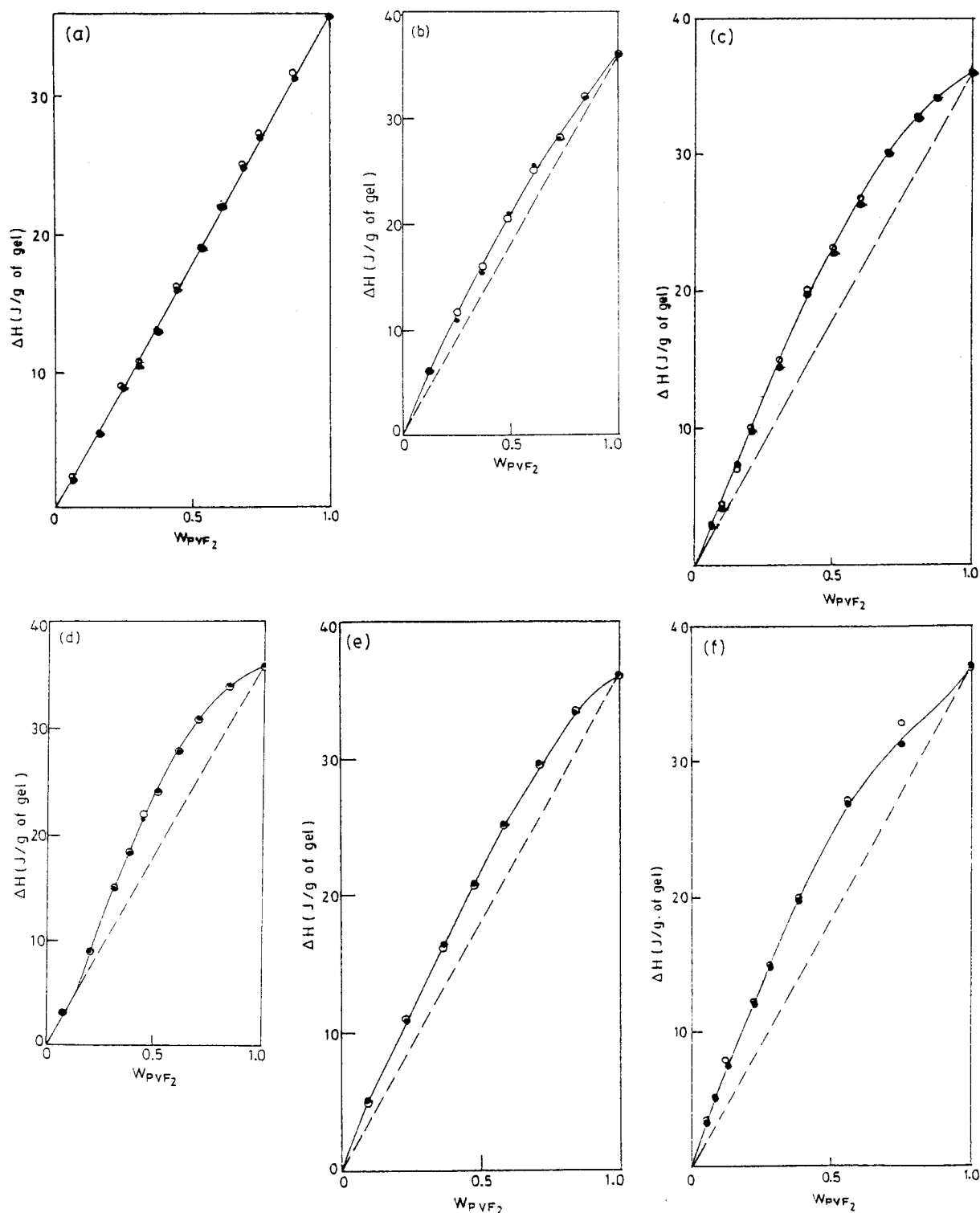


Figure 6. Enthalpy changes during the gel melting/gelation process of PVF₂/diesters gels vs W_{PVF_2} plot (O, melting; ●, gelation): (a) DEO, (b) DEM, (c) DES, (d) DEG, (e) DEP, and (f) DEAZ.

and ΔH_c is the enthalpy for the melting of any polymer-solvent assembled (complex) structure formed during gelation. In the case of the gel formation, the same notation follows where the ΔH represents the enthalpy of formation in each case. Since any of the diesters do not crystallize at the temperature of gelation so at the present case the contribution of the first term is considered as zero. Consequently

$$\Delta H - W_2 \Delta H_2 = \Delta H_c \quad (2)$$

The left-hand side of eq 2 is the positive deviation (Δ) from linearity (Figure 6b-f). The deviation Δ when plotted with W_{PVF_2} usually gives a maximum,^{7,8} and the composition of the maximum gives the composition of the polymer-solvent complex. A representative plot for Δ vs W_{PVF_2} is shown in Figure 7 for the PVF₂/DEG system, and it is apparent from the figure that there is a maximum in the plot. This indicates that there is polymer-solvent complex formation in this gel.^{7,8,20-25} The compositions (W_{PVF_2}) of polymer-solvent complex

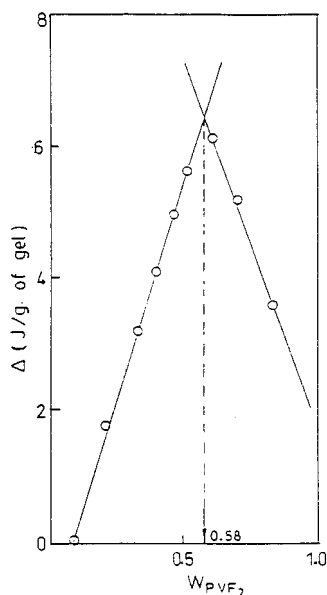
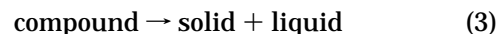


Figure 7. Representative plot for the deviation (Δ) vs W_{PVF_2} of PVF₂ gel in diethyl glutarate (DEG). The arrow indicates the composition of the complex.

formation for PVF₂/DEM, PVF₂/DES, PVF₂/DEG, PVF₂/DEP, and PVF₂/DEA are 0.55, 0.43, 0.58, 0.55, and 0.44, respectively. These correspond to the molar ratios of the PVF₂ monomeric unit and the diesters as 3:1, 2:1, 4:1, 4:1, and 3:1, respectively. Earlier it was shown that a PVF₂–diethyl adipate (DEA) gel also exhibits such polymer–solvent complex formation in a molar ratio of 2:1 for the PVF₂ monomeric unit and the DEA, respectively.⁸ The polymer solvent complex formation may be presumed to occur through the dipole–dipole interaction of the $>C=O$ group of diesters and the $>CF_2$ dipole of PVF₂.^{19,26} So, it may be surmised from these results that polymer solvent complex formation occurs in these diesters $(CH_2)_n < \begin{smallmatrix} COOC_2H_5 \\ COOC_2H_5 \end{smallmatrix}$, where n is greater than zero, but no definite order in the composition of the complex is observed with an increase in the value of n .

In Figure 8a–f the phase diagrams of the gels are shown. Here, both the gel melting temperature (T_{gm}) and the gel formation temperature (T_{gel}) are plotted with W_{PVF_2} . In the case of 100% PVF₂, these are the melting temperature and the crystallization temperature, respectively. The nature of the plot for T_{gm} and T_{gel} is the same, but there is a gap of ~ 30 – 40 °C. It may arise due to the hysteresis effect of the first-order transition⁹ and also due to the use of finite rates. Systems for which the phase diagrams obtained on cooling and on heating are similar can be regarded as formed under equilibrium.²² Hence the phase diagrams may be considered to be of the polymer solvent systems formed under equilibrium. A comparison of the data in the figures reveals that only for PVF₂/DEO gel are the data almost linear, and it is not true for all the other gels, where the deviation from linearity increases with an increase in the chain length of the diesters. Actually the data in these systems can be better drawn in the form of two straight lines or curves as shown in the figures, and they represent the phase diagrams of the polymer–solvent compound formation with different characteristics.^{20–23,25,27} Thus, the phase diagrams of PVF₂/DEM, PVF₂/DES, and PVF₂/DEP gels indicate compound formation with a singular point and PVF₂/DEG and PVF₂/DEAZ gels indicate compound formation

with an incongruent melting point.^{7,8,20,27} In the PVF₂/diethyl adipate (DEA) gel, the phase diagram characteristic is polymer solvent complex formation with an incongruent melting point.⁸ The above phase diagrams are drawn from the endotherms or from the exotherms which show a single peak, and no separate peak for the compound formation occurs in any of the systems in any compositions. So it may be considered that the melting endotherm is actually composed of two indistinguishable peaks: The first of these indistinguishable peaks corresponds to the transformation of



and is nonvariant with composition. The second peak corresponds to the melting of the



and is variant with composition. In the figure the nonvariant transitions are denoted by dotted lines as they are not directly detected in the DSC thermograms.^{7,8} Thus, both the ΔH –composition plot and the phase diagrams support the point that polymer–solvent complex formation occurs in the PVF₂ gels in diesters except in the diethyl oxalate. As presented earlier the FT-IR spectra and WAXS pattern also show existence of new peaks for complex formation except in DEO. However, the occurrence of a new peak in the WAXS pattern at 3.09 Å for the PVF₂/DEO system is not clear to us. The polymer solvent complex formation inhibits the chain-folding process, yielding fibrillar crystallites. A polymer chain passes through many such fibrils, and these fibrils entrap the solvent to produce the gel. On the other hand, in the PVF₂/DEO system, the polymer chains obtained by a chain-folding process constitute the spheroids which entrap the solvent to produce the gels. These mechanisms of gelation are different from that of the rodlike polymers where the end to end aggregation of the chain entraps the solvent to produce the gel.²⁸

Molecular Modeling. An approximate idea of the polymer–solvent complex formation is done here through molecular mechanics calculation with the help of the MMX method²⁹ using a personal (Pentium) computer. For this purpose, we have minimized energetically the α -phase PVF₂ and we have also energetically minimized the solvent molecule, separately. The conformation of the solvent molecule is set to get the compound of desired composition as obtained from thermodynamic study. Then by combining the two polymer and the two solvent molecules at alternate positions, we again minimize the whole system, to form the complex in the gaseous phase. After minimization through the MMX program, we have queried the distance between the carbon atom of the $>CF_2$ group and the oxygen atom $>C=O$ of carbonyl group. This is done because there is some dipolar interaction between the $>C=O$ group and the $>CF_2$ unit of PVF₂, as mentioned earlier.^{19,26} The above distances are presented in Table 3, and it is apparent from the table that the distances are equal to or below 3.65 Å in all cases. The van der Waals radius of the $>CF_2$ group is 2.25 Å³⁰ and that of oxygen is 1.4 Å,³¹ so the distance of interatomic contacts between the $>CF_2$ group and the oxygen of the $>C=O$ group would be 3.65 Å. Therefore, it may be argued that polymer solvent complex formation is primarily supported by molecular mechanics in all the PVF₂/diester systems. This molecular modeling, therefore, concludes that the

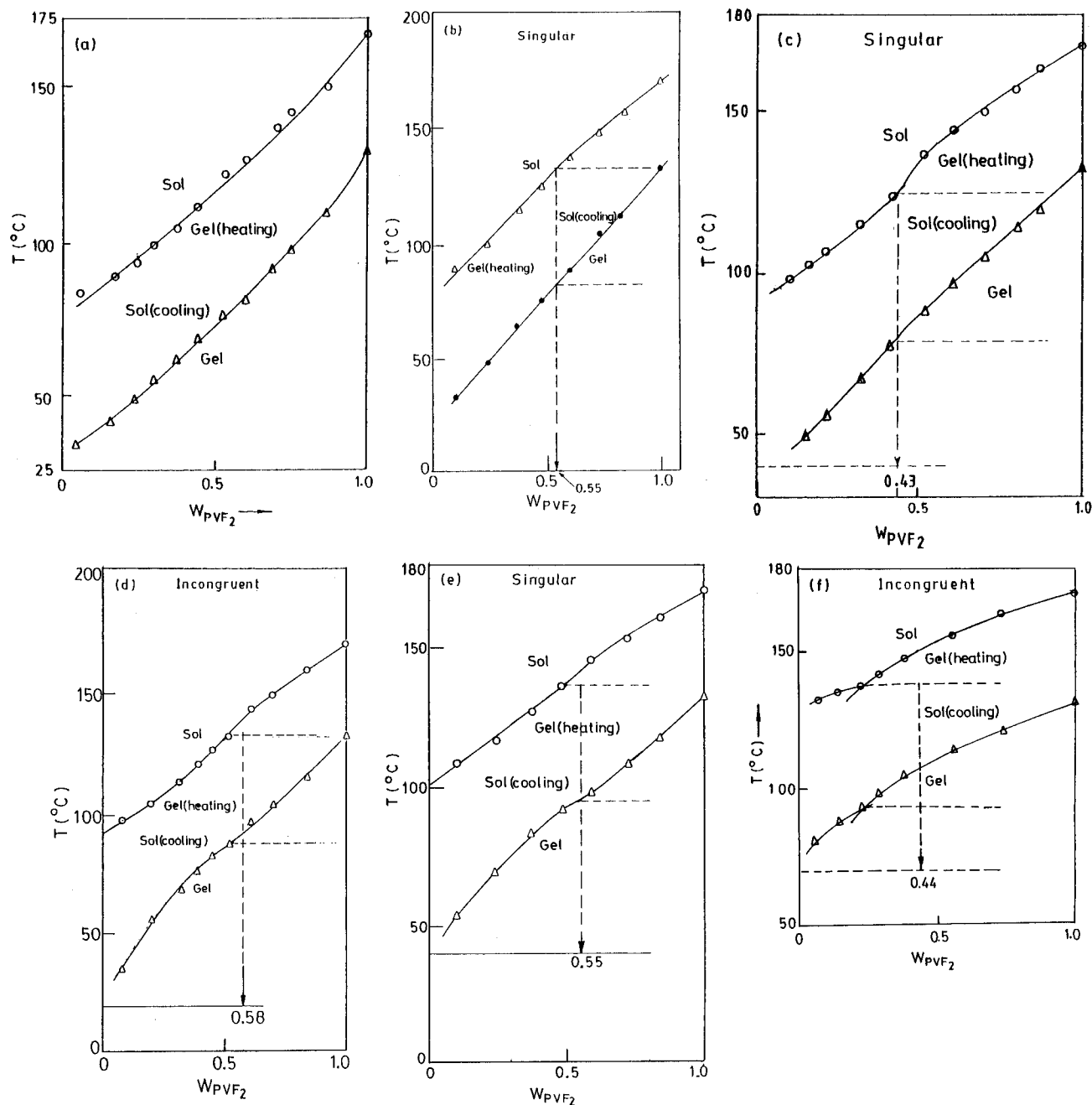


Figure 8. Gel melting temperature and the gelation temperature vs W_{PVF_2} plot of PVF_2 gels in diesters (O, gel melting; Δ , gelation): (a) DEO, (b) DEM, (c) DES, (d) DEG, (e) DEP, and (f) DEAZ. (The intermediate regions between gel melting and gelation temperatures are due to the hysteresis effect. It is gel during heating a gel and sol during cooling a solution.)

Table 3. Interatomic Distance of Carbonyl Oxygen and the $>\text{CF}_2$ Group of Diesters and PVF_2 , Respectively, Obtained from Molecular Modeling Using a MMX Program

diesters	composition of the complex diester:monomer	nature of complexation	interatomic distance $\text{C}=\text{O} \cdots >\text{C}^*\text{F}_2$ (Å)
DEO	1:2	intermolecular	3.54, 3.61, 3.35
DEM	1:3	intramolecular	3.66, 3.51, 3.38, 3.54
DES	1:2	intermolecular	3.48, 3.35, 3.53
DEG	1:4	intermolecular	3.48, 3.36, 3.41
DEA	1:2	intermolecular	3.64, 3.48, 3.10
DEP	1:4	intermolecular	3.09, 2.60, 2.59
DEAZ	1:3	intramolecular	2.99, 3.21, 2.99, 3.21

polymer-solvent complexation is also possible in a PVF_2/DEO gel. The polymer solvent clathrate com-

pounds may be intramolecular or intermolecular. The former means that the diester molecule is forming the complex with the same PVF_2 chain while the later indicates that the diester molecule makes the complex with two PVF_2 chains side by side. A typical example of both types of complexes is shown in Figure 9 a,b. The structure of the complexes produced in the gel may not be exactly the same due to the packing in the crystal lattice, but the approximation may be made that they will not be much different from those found in the molecular modeling. Such solvent complexed polymer chains combine together to form the fibrils.

Discussion. The disparity between the molecular modeling and thermodynamic/morphological study in the PVF_2 -DEO gel may be due to the smallest size of the DEO compared with those of the other diesters.

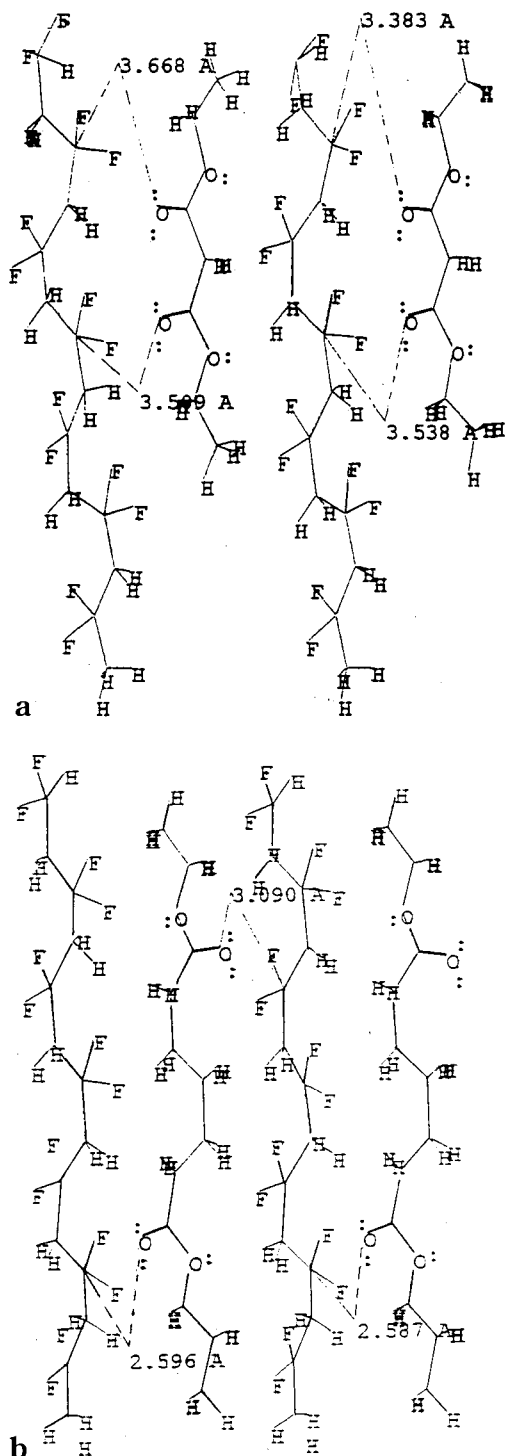


Figure 9. Molecular models of PVF₂ (α-polymorph) gels in diesters representing intramolecular and intermolecular polymer-solvent complex formation. The distances between carbonyl oxygen and carbon atom of the >CF₂ group are shown. Key: (a) PVF₂/DEM (intramolecular) and (b) PVF₂/DEP (intermolecular) gels.

Because of its smallest size and lowest molecular weight, its thermal movement is more frequent than those of the others in the sol/gel state. This easier thermal movement probably inhibits its physical binding with the >CF₂ dipoles of the polymer chain and thereby fails to produce the complex. Also the enthalpy of polymer-solvent complex formation may depend on the size of the diester. The mixed morphology of the PVF₂/DEM system containing both fibrils and spheroids

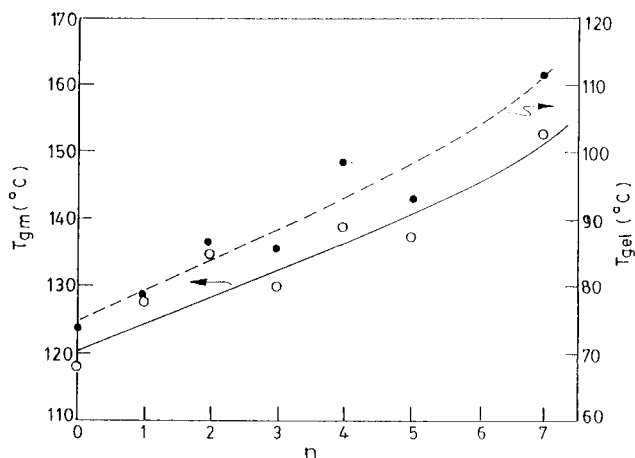


Figure 10. T_{gm} and T_{gel} vs number of intermittent carbon atoms (n) of diesters of PVF₂ gels in diesters for $W_{PVF_2} = 0.5$ (obtained from Figure 8): ○ = T_{gm} ; ● = T_{gel} .

as observed in both SEM and TEM pictures may also be explained similarly. Since the number of intermittent carbon atom increases by one from DEO, so the mobility of DEM in sol/gel state somewhat decreases than that of DEO system. This may cause an equilibrium containing both complexed and uncomplexed PVF₂ chains, producing borderline morphology. These uncomplexed PVF₂ chains produce spheroids in the gel. With a further increase in the " n " value, due to lesser mobility of diesters, the complexation is almost complete and fibrillar morphology is observed. No doubt, the texture of the fibrils is more distinct with an increase in the value of " n ", and the PVF₂/DEAZ gel shows the finest fibrils in these series, since it has the least mobility in the series.

Possible support for the above assertion may come from Figure 10 where gel melting (T_{gm}) and gelation (T_{gel}) temperatures are plotted with the number of intermittent carbon atoms " n " of the diesters at a particular composition ($W_{PVF_2} = 0.5$). The T_{gm} and T_{gel} values are computed from the phase diagrams shown in the Figure 8. It is apparent from the Figure 10 that with an increase in " n ", the T_{gm} or T_{gel} increases almost linearly. This is because when " n " is smaller the mobility of the solvent molecules in the gel network is high. Consequently, by a small increase in the temperature, the solvent mobility increases and breaks the physical network structure easily. However, for larger size solvent molecules, the solvent mobility is low in the gel, and it requires a greater temperature to break the physical network. Similarly, during gelation, the larger size solvent molecules in the sol state have lesser mobility than that of the smaller ones and easily produce gels.

Apart from the above entropic explanation of gel behavior, the enthalpic contribution is also playing an important role. In Figure 11, a plot of enthalpy of complexation ΔH_c against the number of intermittent carbon atoms " n " are shown. (ΔH_c values are obtained from Figure 7 at the maxima). Though the data points are somewhat scattered, it is apparent from the figure that ΔH_c increases with an increase in " n ". A probable reason is that the polarizability of the >C=O group increases with an increase in " n ",³² and this causes a stronger interaction between the >C=O group of the diester and the >CF₂ unit of the PVF₂ chain. Thus, with increasing n the polymer-solvent complex becomes

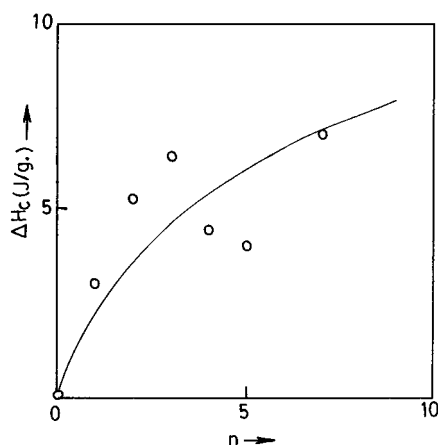


Figure 11. Enthalpy of complexation (ΔH_c) vs number of intermittent carbon atoms (n) of diesters of PVF₂ gels in diesters.

more stronger and for $n > 1$ we observe fibrillar-like morphology. When $n = 7$, due to the strongest interaction in the series, distinct fibrils are observed. Thus, the intermittent lengths of the diester have both enthalpic and entropic contributions to polymer solvent complexation.

Conclusion. The PVF₂ produces thermoreversible gels in diesters of varying numbers of intermittent methylene groups ($n = 0-7$). The gel consists of α -phase PVF₂ crystals in all the diesters studied here. The morphology of the gel is spheroidal when $n = 0$; $n = 1$ gels have a mixed morphology, but when $n > 1$ the morphology is fibrillar-like. The enthalpy of gel melting and the enthalpy of gel formation vs composition plot indicate polymer solvent complex formation for diesters with $n \geq 1$. The compound formation inhibits the chain-folding process, producing fibrillar gels. For $n = 1$, the compound formation is not complete, yielding mixed morphology. The stoichiometries of the complexes with respect to the diesters and the PVF₂ monomeric units are 3:1, 2:1, 4:1, 2:1, 4:1, and 3:1 for PVF₂-DEM, PVF₂-DES, PVF₂-DEG, PVF₂-DEA, PVF₂/DEP, and PVF₂/DEAZ gels, respectively. The phase diagrams also indicate polymer-solvent compound formation with a singular point for PVF₂-DEM, PVF₂-DES, and PVF₂/DEP gels and with an incongruent melting point for PVF₂-DEG gels and PVF₂/DEAZ gels. The molecular mechanics calculation concludes that for all the diesters ($n = 0-7$), polymer-solvent compound formation is possible. However, the disparity between the molecular modeling and the morphological and thermodynamical investigations in PVF₂-DEO gel may be due to the smaller size of DEO than the other diesters. The borderline morphology of PVF₂-DEM system is also due to the same reason. With an increase in the intermittent carbon atom (n), the fibrillar texture becomes more distinct. T_{gm} and T_{gel} increase with an increase in " n "

at a particular composition, and ΔH_c also increases with an increase in " n ", suggesting that there is both enthalpic and entropic contributions from intermittent length of the diester on the polymer-solvent complexation.

References and Notes

- (1) *Reversible Polymeric Gels and Related Systems*; Russo, P. S., Ed.; ACS Symposium Series; American Chemical Society: Washington, DC, 1986.
- (2) Guenet, J. M. *Thermoreversible Gelation of Polymers and Biopolymers*; Academic Press: London, 1992.
- (3) Wang, T. T.; Herbert, J. M.; Glass, A. M. *In the Application of Ferroelectric Polymers*; Blackie & Sons Ltd.: London, 1988.
- (4) Cho, J. W.; Song, H. Y.; Kim, S. Y. *Polymer* **1993**, *34*, 1024.
- (5) Mal, S.; Maiti, P.; Nandi, A. K. *Macromolecules* **1995**, *28*, 2371.
- (6) Mal, S.; Nandi, A. K. *Polymer* **1998**, *39*, 6301.
- (7) Mal, S.; Nandi, A. K. *Langmuir* **1998**, *14*, 2238.
- (8) Dikshit, A. K.; Nandi, A. K. *Macromolecules* **1998**, *31*, 8886.
- (9) Daniel, C.; Dammer, C.; Guenet, J. M. *Polymer* **1994**, *35*, 4243.
- (10) Lovinger, A. J. In *Developments in Crystalline Polymers-1*; Basset, D. C., Ed.; Elsevier Applied Science: London 1981; p 195.
- (11) Prest, W. M., Jr.; Luca, D. J. *J. Appl. Phys.* **1975**, *46*, 4238.
- (12) Lando, J. B.; Doll, W. W. *J. Macromol. Sci. Phys.* **1968**, *2* (2), 205.
- (13) Hasegawa, R.; Takahashi, Y.; Chatani, Y. *Polym. J.* **1972**, *3*, 600.
- (14) Bechmann, M. A.; Lando, J. B. *Macromolecules* **1981**, *14*, 40.
- (15) Sundararajan, P. R.; Tyrer, N. J.; Bluhm, T. L. *Macromolecules* **1982**, *15*, 286.
- (16) Cortili, G.; Zebri, G. *Spectrochem. Acta* **1967**, *23A*, 2218.
- (17) Enomoto, S.; Kawai, Y.; Sugita, M. *J. Polym. Sci.* **1968**, *A26*, 861.
- (18) Kobayashi, M.; Tashiro, K.; Tadokoro, H. *Macromolecules* **1975**, *8*, 158.
- (19) Belke, R. E.; Cabasso, I. *Polymer* **1988**, *29*, 1831.
- (20) Guenet, J. M.; McKenna, G. B. *Macromolecules* **1988**, *21*, 1752.
- (21) Spevacek, J.; Saiani, A.; Guenet, J. M. *Macromol. Rapid Commun.* **1996**, *17*, 389.
- (22) Guenet, J. M. *Thermochem. Acta* **1996**, *284*, 67.
- (23) Ramzi, M.; Rochas, C.; Guenet, J. M. *Macromolecules* **1996**, *29*, 4668.
- (24) Guenet, J. M. *Macromolecules* **1987**, *20*, 2874.
- (25) Saiani, A.; Spevacek, J.; Guenet, J. M. *Macromolecules* **1998**, *31*, 703.
- (26) Roerdink, E.; Challa, G. *Polymer* **1980**, *21*, 509.
- (27) Reisman, A. *Phase Equilibria*; Academic Press: New York, 1970.
- (28) Tipton, D. L.; Russo, P. S. *Macromolecules* **1996**, *29*, 7402.
- (29) Gajewski, K. E.; Gilber, Mckelvie, H. In *Advances in Molecular Modeling*; Liotta, D., Ed.; JAI Press: Greenerick, CT, 1990; Vol. 2.
- (30) The van der Waals radius of the $>CH_2$ group is 2.0 Å, and those of hydrogen and fluorine are 1.2 and 1.35 Å, respectively.³¹ Therefore, by the approximation of the increment of the van der Waals radius of 12.5% due to replacement of hydrogen by fluorine atom, the van der Waals radius of the $>CF_2$ group is 2.25 Å.
- (31) Pauling, L. *The Nature of Chemical bond, and the structure of molecules and crystals*, 3rd ed.; Cornell University Press: Ithaca, NY, 1960; p 257.
- (32) Najeh, M.; Munch, J. P.; Guenet, J. M. *Macromolecules* **1992**, *25*, 7018.

MA990898G